

## Article

# Extraction of Aquaculture Pond Region in Coastal Waters of Southeast China Based on Spectral Features and Spatial Convolution

Lin Wang<sup>1,2,3</sup>, Yefan Li<sup>1,2,3</sup>, Dongzhu Zhang<sup>1,2,3</sup> and Zhicai Liu<sup>1,2,3,\*</sup>

<sup>1</sup> College of Environmental and Safety Engineering, Fuzhou University, Fuzhou 350108, China; wanglin@fzu.edu.cn (L.W.); n190620011@fzu.edu.cn (Y.L.); 200620006@fzu.edu.cn (D.Z.)

<sup>2</sup> Academy of Geography and Ecological Environment, Fuzhou University, Fuzhou 350108, China

<sup>3</sup> Fujian Provincial Key Laboratory of Remote Sensing of Soil Erosion and Disaster Prevention, Fuzhou 350108, China

\* Correspondence: lczlzc@fzu.edu.cn

**Abstract:** To control the negative effects resulting from the disorderly development of aquaculture ponds and promote the development of the aquaculture industry, rapid and accurate identification and extraction techniques are essential. An aquaculture pond is a special net-like water body divided by complex roads and dikes. Simple spectral features or spatial texture features are not sufficient to accurately extract it, and the mixed feature rule set is more demanding on computer performance. Supported by the GEE platform, and using the Landsat satellite data set and corresponding DEM combined with field survey data, we constructed a decision-making model for the extraction of aquaculture ponds in the coastal waters, and applied this method to the coastal waters of Southeast China. This method combined the image spectral information, spatial features, and morphological operations. The results showed that the total accuracy of this method was 93%, and the Kappa coefficient was 0.86. The overlapping proportions of results between the automated extraction and visual interpretation for test areas were all more than 90%, and the average was 92.5%, which reflected the high precision and reliability of this extraction method. Furthermore, in 2020, the total area of coastal aquaculture ponds in the study area was 6348.51 km<sup>2</sup>, which was distributed primarily in the cities of Guangdong and Jiangsu. Kernel density analysis suggested that aquaculture ponds in Guangdong and Jiangsu had the highest degree of concentration, which means that they face higher regulatory pressure in the management of aquaculture ponds than other provinces. Therefore, this method can be used to extract aquaculture ponds in coastal waters of the world, and holds great significance to promote the orderly management and scientific development of fishery aquaculture.



**Citation:** Wang, L.; Li, Y.; Zhang, D.; Liu, Z. Extraction of Aquaculture Pond Region in Coastal Waters of Southeast China Based on Spectral Features and Spatial Convolution. *Water* **2022**, *14*, 2089. <https://doi.org/10.3390/w14132089>

Academic Editor: Fernando António Leal Pacheco

Received: 29 May 2022

Accepted: 25 June 2022

Published: 29 June 2022

**Publisher's Note:** MDPI stays neutral with regard to jurisdictional claims in published maps and institutional affiliations.



**Copyright:** © 2022 by the authors. Licensee MDPI, Basel, Switzerland. This article is an open access article distributed under the terms and conditions of the Creative Commons Attribution (CC BY) license (<https://creativecommons.org/licenses/by/4.0/>).

**Keywords:** aquaculture pond area; threshold segmentation; spatial convolution; GEE platform

## 1. Introduction

According to the 2020 edition of statistics released by the Food and Agriculture Organization of the United Nations, global fishery has been developing rapidly, with total output increasing by 42% from 2000 to 2018 [1]. As the main driving force of fishery growth, aquaculture had an average annual growth trend of 5.3% from 2000 to 2018, and production peaked at 82.1 million tons in 2018 [1]. China is the largest aquaculture country in the world [1]. In the past, catch production has occupied the dominant position in total fishery production. With the growing population's demand for food and nutrition, and the growing need for the protection and sustainable development of fish germplasm resources, the aquaculture industry has developed rapidly. After the reform and opening up, the focus of China's fisheries gradually shifted from fishing to aquaculture, and China became one of the few countries in the world where aquaculture output is much higher than the

amount of fishing [2–4]. Additionally, China has the highest aquaculture output, and is, globally, the largest aquaculture exporter [1].

Aquaculture ponds in the coastal zone are the main bearing form of aquaculture. With the rapid development of aquaculture, coastal aquaculture ponds have introduced considerable economic benefits. As a transitional area between sea and land, these coastal areas have valuable natural resources, and their ecosystems are vulnerable. Therefore, aquaculture not only brings economic benefits to coastal areas, but also brings environmental protection problems to coastal ecosystems. The problems include increased management difficulties, unreasonable layouts [5], overcapacity and overplanning of aquaculture systems [6], and aquaculture sewage discharge and carbon emissions, which have introduced increasingly negative effects on the region's environment. To control the negative effects brought about by this disorganized development, and to promote the further development of the aquaculture industry, it is essential to identify and extract aquaculture ponds quickly and accurately.

Because of manpower limitations, material resources, and accessibility, traditional fishery field investigation is time-consuming and laborious. The official fishery statistics have only classified aquaculture areas, making it difficult to reflect the spatial distribution and spatiotemporal cooperative change trends of objects from a macro perspective. Therefore, remote sensing technology, which can achieve high precision in a short period, as well as large-area synchronous monitoring, has become a stable and reliable technical means for fishery investigation. Visual interpretation is a classical method used to extract aquaculture areas from remote sensing images [7–10], but its operation is subjective, and the interpreter's prior knowledge has a significant influence on extraction accuracy, resulting in low efficiency. Using spectral features, some scholars have tried to automatically extract aquaculture areas according to spectral classification [11–18], or by constructing a spectral feature index [19–23]. Spectral classification, however, is susceptible to the phenomenon of "same object different spectrum" and "foreign object in the same spectrum", and the spectral characteristic index is constructed primarily for a certain region or a certain sensor, which has low portability and robustness. In recent years, object-oriented extraction methods have been used widely [24–31], and scholars usually use multiscale segmentation to establish feature rule sets that combine shape, spectrum, and texture information to achieve automatic extraction. This calculation, however, requires a lot of system resources and has strict requirements on computer performance, as well as on the quantity and quality of remote sensing images. Therefore, efficient, reliable, and accurate aquaculture pond extraction schemes remain a major challenge.

Google Earth Engine (GEE) is a cloud-based platform that can efficiently process large-scale geospatial data sets. Because GEE contains free public image data obtained from various satellite sensors [32], it greatly reduces the threshold of a massive data analysis system and breaks through the bottleneck of multisource remote sensing data acquisition. Therefore, scholars have begun carrying out their research on the GEE platform [33–38]. It is evident that the research on aquaculture ponds based on the GEE cloud platform has broad application prospects.

To solve the problem of low efficiency, weak robustness, and strict requirements on computer performance in the existing extraction methods, and to achieve the goal of more efficient and accurate identification of aquaculture ponds, we proposed an automatic extraction method for coastal aquaculture ponds combining spectral information, spatial features, and morphological operation based on the GEE platform. This method can be used to accurately identify and evaluate the aquaculture ponds and their spatial distribution in southeast coastal areas, and provides theoretical reference and data support to effectively reduce the difficulty of coastal breeding pond management, to significantly control the negative impacts of aquaculture ponds on the environment, and to protect marine water quality.

## 2. Study Area and Data Sources

### 2.1. Study Area

The southeast coast of China stretches from Jiangsu in the north to Hainan in the south, Guangxi in the west, and Taiwan in the east, which consists of eight provinces, two special administrative regions, one autonomous region, and one municipality directly under the central government. The north–south span is about 1800 km, and the east–west span is about 1500 km. The region has abundant water resources and a developed river network, forming coastal plains, such as the Yangtze River Delta and Pearl River Delta, as well as abundant tidal flats and shallow water bays. Therefore, it offers a distinct advantage in the large-scale construction of aquaculture ponds. The southeast coastal area has a long coastline. Jiangsu, Zhejiang, Fujian, and Guangdong in the region are famous aquatic provinces in China. In 2020, the total area of fishery farming was 27,028.80 km<sup>2</sup>, accounting for 38.41% of China’s fishery farming. The total output value of the fishery economy was 1650.356 billion yuan, accounting for 59.92% of the national total output value of the fishery economy, among which, the output value of fishery breeding was 611.337 billion yuan, accounting for 45.23% of the national total output value of the fishery economy. The research area included the coastal cities of five provinces (Jiangsu, Zhejiang, Fujian, Guangdong, and Guangxi), one municipality directly under the central government (Shanghai), and the main island of Hainan Island, which has coastal zone breeding conditions in southeast China (Figure 1). We conducted aquaculture pond automatic recognition and extraction algorithm research, and analyzed the spatial agglomeration features of this study area.

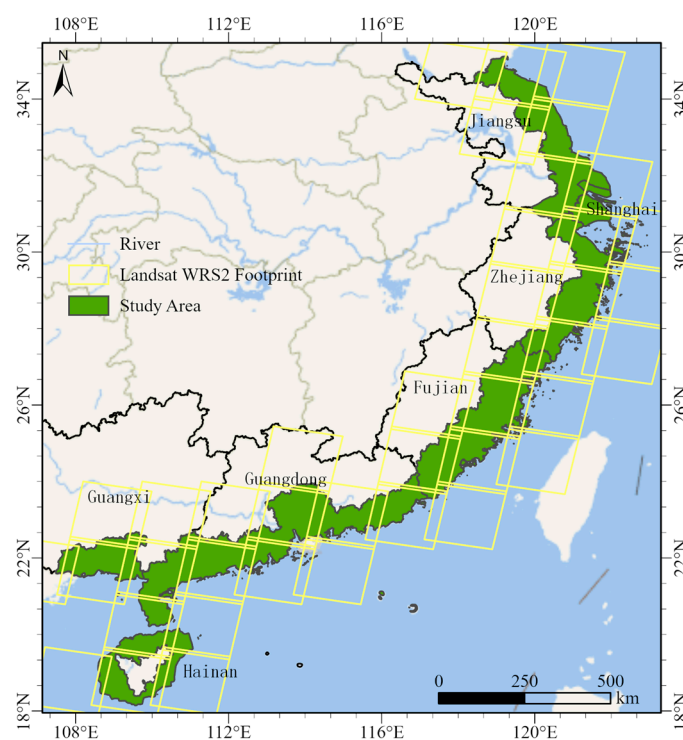


**Figure 1.** Study area.

In this study, the extracted aquaculture pond refers to artificial or semi-artificial open ponds that are distributed in coastal areas for aquaculture purposes. Ponds are bound by roads or embankments with different widths, which, generally, are presented in the form of regular or irregular grids in remote sensing images. Aquaculture pond water consists of brackish or freshwater, and its spectral characteristics are similar to a water body. Google images of typical aquaculture ponds and their corresponding field survey photos are shown in Figure 2.

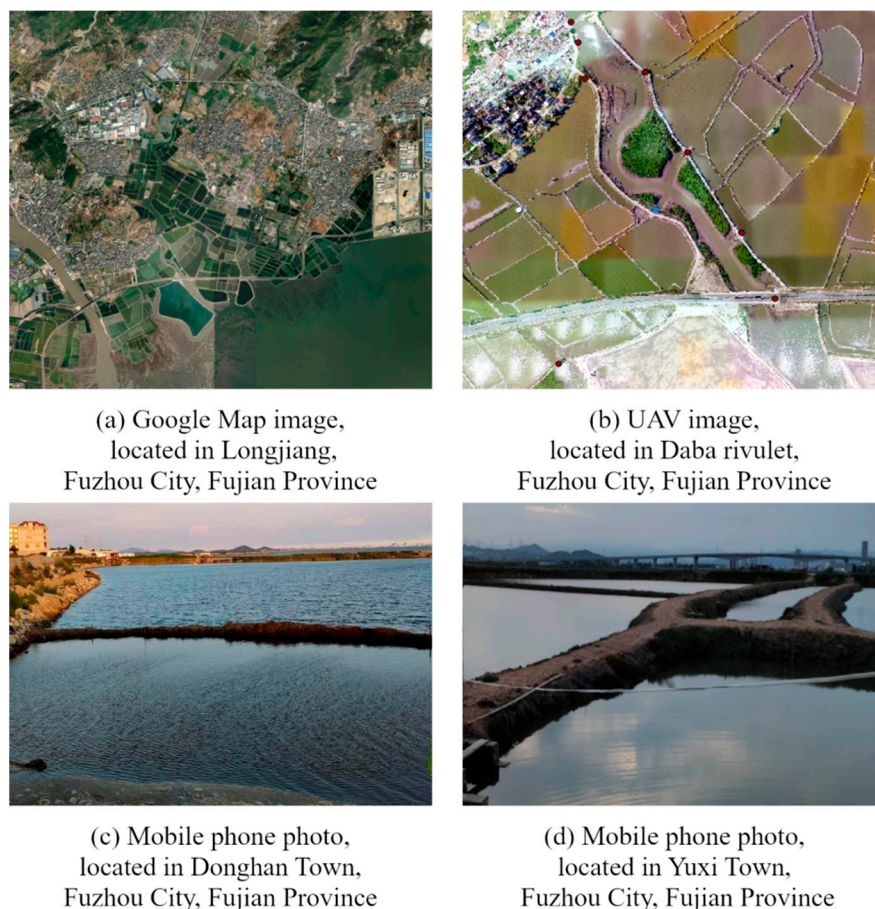


**Figure 2.** Objects of an aquaculture pond in remote sensing images and in situ photos.

## 2.2. Data Sources

In this study, we used data from Landsat series remote sensing images from the U.S. Geological Survey (USGS), with a spatial resolution of 30 m and a reentry period of 16 d. The GEE platform code can directly call the Landsat image covering the study area after atmospheric correction (the code of GEE internal retrieval is `Landsat /LC08/C02/T1_L2`), and the preprocessing processes, such as Mosaic and cutting, can also be completed on this platform. As aquaculture ponds, generally, are drained and cleaned in spring and winter [39], we set the image collection time between March and October 2020 to avoid the dry pond period as much as possible [40,41]. Additionally, we used the quality assessment band to eliminate the influence of clouds and cloud shadows, and finally, we obtained Landsat-8 remote sensing images covering the study area.

In addition, we obtained the digital elevation model (DEM) data used in this study from the National Aeronautics and Space Administration (NASA). NASA's SRTM (Shuttle Radar Probe Mission) V3 (SRTM Plus) offers a spatial resolution of 1 arc-second (approximately 30 m). It can be called directly from the GEE platform by code (the internal fetching code of GEE is `USGS/SRTMGL1_003`). Other basic geographic data involved in the study came from the National Geographic Information Center's 1:400,000 map database.

## 3. Research Methods

Supported by the GEE platform and using the Landsat satellite data set and corresponding DEM in the study area combined with field survey data, we constructed a decision-making model for the extraction of aquaculture ponds in the coastal waters of the study area (Figure 3). The process can be summarized as follows: (1) delineation of aquaculture coverage area supported by DEM; (2) elimination of non-water information based on morphological and spectral features; (3) elimination of non-aquaculture water

body information based on spatial convolution; and (4) postprocessing. In the study area, we selected two typical aquaculture pond areas as test areas to show the process and effect of step-by-step extraction.

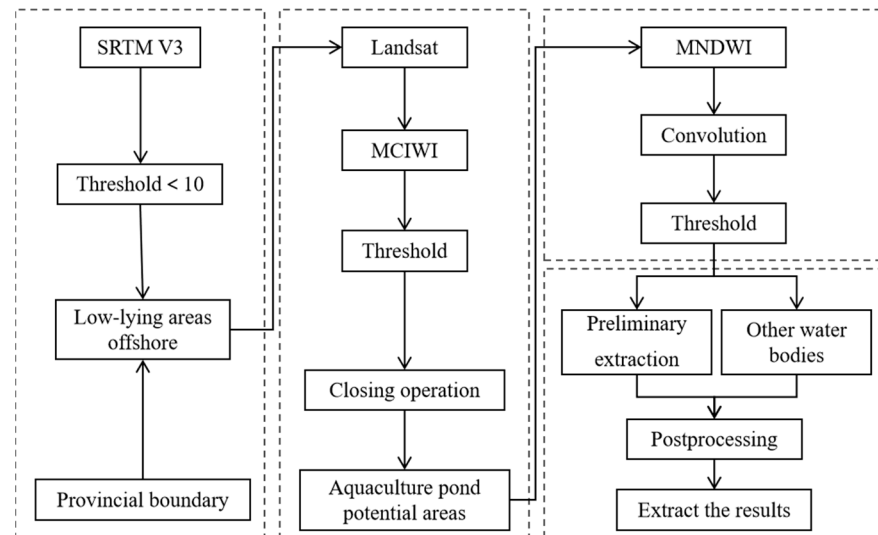


**Figure 3.** Flowchart of the aquaculture pond region extraction procedure (MCIWI: Modified Combined Index for Water Body Identification; MNDWI: Modified Normalized Difference Water Index).

### 3.1. Delineation of Aquaculture Coverage Area Supported by DEM

Because offshore aquaculture ponds are distributed primarily along the gentle coastal zone, SRTM elevation data could be used to mask the inland higher altitude areas, with 10 m as the threshold [42]. As a result, we could determine the potential coverage area of the distribution of the aquaculture ponds. The objects acquired through this step are composed of non-water information (such as buildings, vegetation, or tidal flats) in gentle coastal zones, as well as water information, such as the surface of aquaculture ponds or seawater. As shown in Figure 4, test areas A and B are composed mainly of the central water system and the aquaculture ponds attached to the water system, and the surrounding areas are covered with buildings, bare soil, and vegetation. After the SRTM elevation threshold mask, only the hydrographic net, the water surface of aquaculture ponds, and a small part of the low-elevation bare soil, vegetation, and building information were reserved (Figure 4c,f).

### 3.2. Elimination of Non-Water Information Based on Morphological and Spectral Characteristics

After obtaining the coverage area of the aquaculture pond, we removed the remaining non-water information, including bare soil, vegetation, and buildings in the low-altitude area. Remote sensing water index has been the main technology used to extract water surface information from remotely-sensed imagery, and to distinguish the boundary between land and water. According to the land use type and land cover characteristics of the coastal zone, we used the Modified-Combined Index for Water Body Identification (MCIWI) [43] to remove the non-water information in the aquaculture coverage area. We used Otsu's [44] method, an algorithm to determine the threshold of binary image segmentation, which is also known as the maximum interclass variance method, to perform automatic threshold segmentation.

The MCIWI index combines normalized difference building index (NDBI) and normalized difference vegetation index (NDVI). NDVI is sensitive to vegetation, such as forest land and arable land, and can eliminate some effects of thin clouds and radiation. NDBI highlights the characteristics of construction land, and can enhance differences between water bodies and non-water bodies, such as buildings and vegetation. The formula is as follows:

$$MCIWI = NDVI + NDBI = \frac{(NIR - RED)}{(NIR + RED)} + \frac{(MIR - NIR)}{(MIR + NIR)}, \quad (1)$$

where *RED* is the reflectance of the red light band of the image, *NIR* is the reflectance of the near-infrared band of the image, and *MIR* is the reflectance of the middle infrared band of the image.

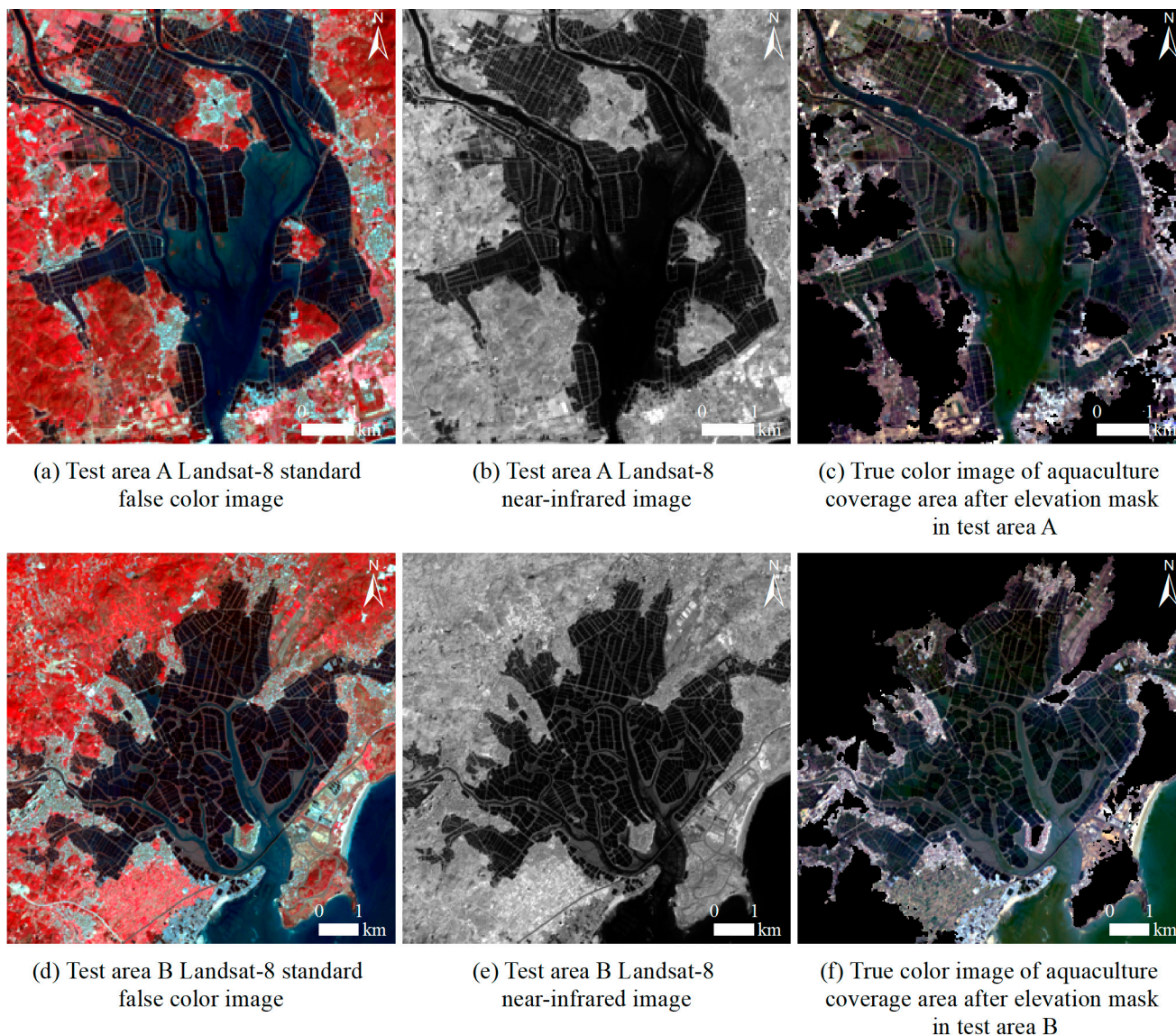


**Figure 4.** Delineation of potential aquaculture coverage areas in test area A (B).

Figure 5 shows the ability of the *MCIWI* index to distinguish between water body and non-water-body information in the study area. We selected 200 random points for each of the surface cover types of the coastal zone, such as water bodies, vegetation, buildings, and bare soil, and we extracted and counted the *MCIWI* values of random points. The *MCIWI* values of most water bodies were in the range of  $(-1, 0)$ . In contrast, *MCIWI* values of non-water-body information, such as vegetation, buildings, and bare soil, were all greater than 0, which reflected the separability and feasibility of automatic threshold segmentation from water information.

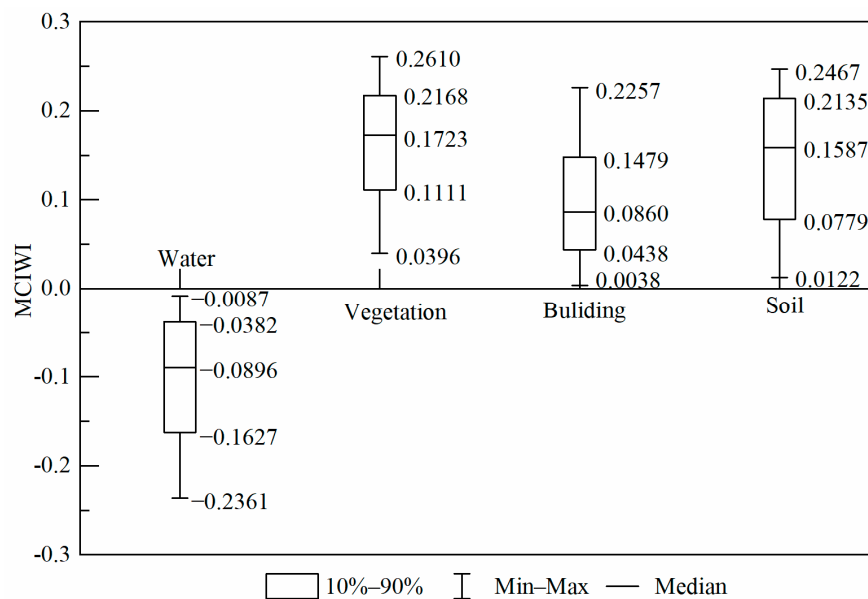


Figure 5. Comparison of MCIWI values of water body and non-water-body information in the study area.

Otsu’s method is an automatic threshold segmentation algorithm based on the first-order statistical characteristics of the gray histogram. This method is not affected by image brightness and contrast, has fast operation speed and high storage efficiency, and is widely used in the research of image threshold segmentation [45,46]. We used Otsu’s method to obtain the optimal threshold of water and non-water segmentation in the test area. The MCIWI results (Figure 6a,d) were binarized to determine the water–land boundary (Figure 6b,e). We performed a morphological closure operation to remove the unconnected cavities in the aquaculture water, and obtained the water coverage area (Figure 6c,f).

### 3.3. Information Elimination of Non-Aquaculture Water Body Based on Spatial Convolution

The water information obtained in the previous step included aquaculture pond water and non-aquaculture water. The key aspect of this step was to distinguish between these two types of water. The spectral reflectance of the water body was low, the spectral response was weak, and the extraction accuracy was not high. It was more difficult to distinguish one type of water body from another type of water body because this required a targeted recognition method to enhance spectral differences to achieve effective separation.

Since the modified normalized difference water index (MNDWI) [47] was proposed, it has been one of the most cited water indexes in practice and research because of its fine water discrimination. The formula is as follows:

$$MNDWI = \frac{GREEN - MIR}{GREEN + MIR} \tag{2}$$

where GREEN represents the reflectance of the green light band of the image, and MIR represents the reflectance of the mid-infrared band of the image.

In this study, we used the MNDWI to enhance the low-reflection information of aquaculture ponds, and to improve the clarity of the grid characteristics of aquaculture ponds. We selected 200 random points from aquaculture and non-aquaculture water bodies in the study area, and extracted and counted the MNDWI values of random points (Figure 7). Under the action of the MNDWI, most aquaculture-related water bodies could be distinguished from non-aquaculture-related water bodies, but within the MNDWI interval of 0.1139–0.1194, it is still challenging to distinguish.

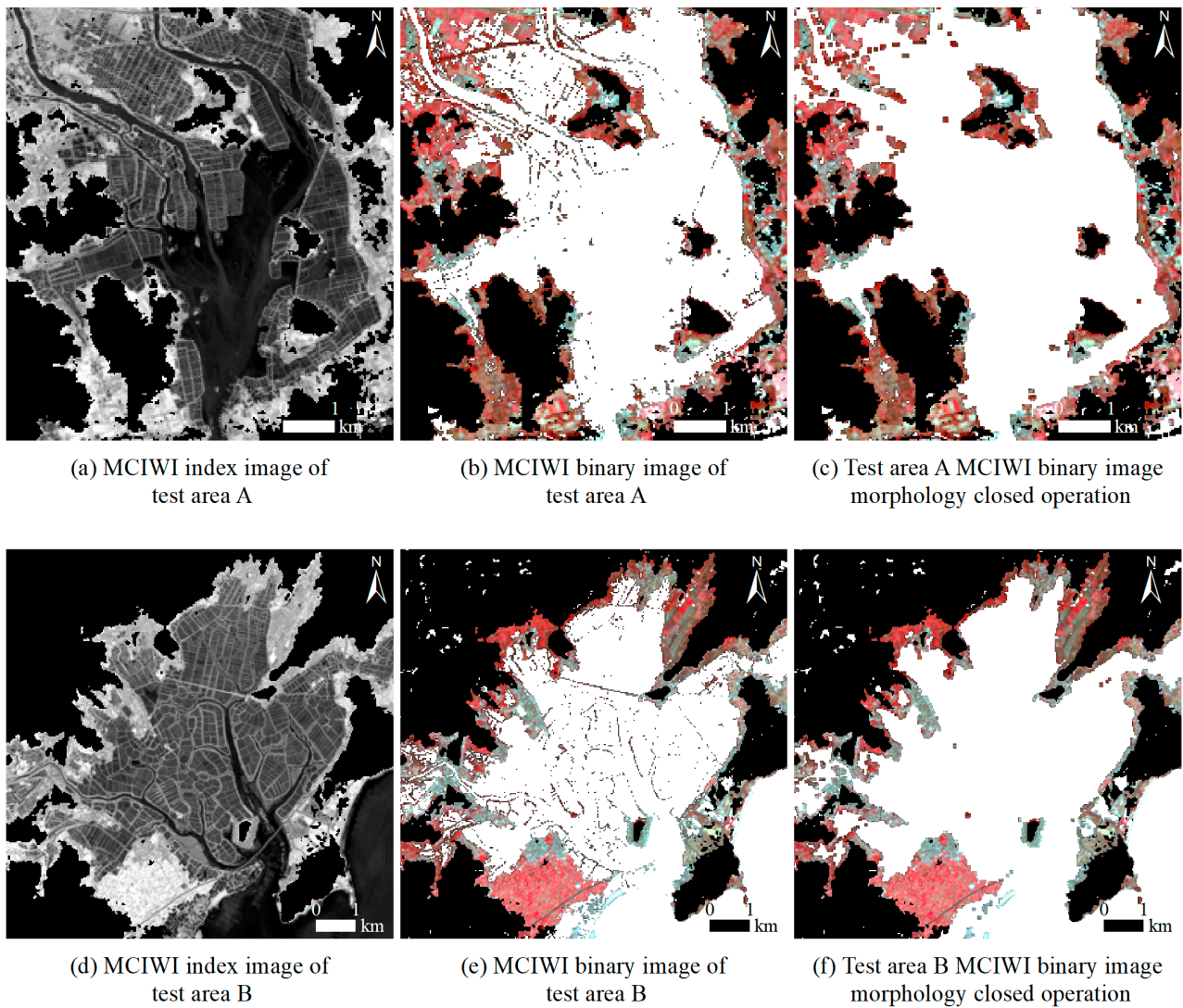


Figure 6. Elimination of non-water-body information in test area A (B).

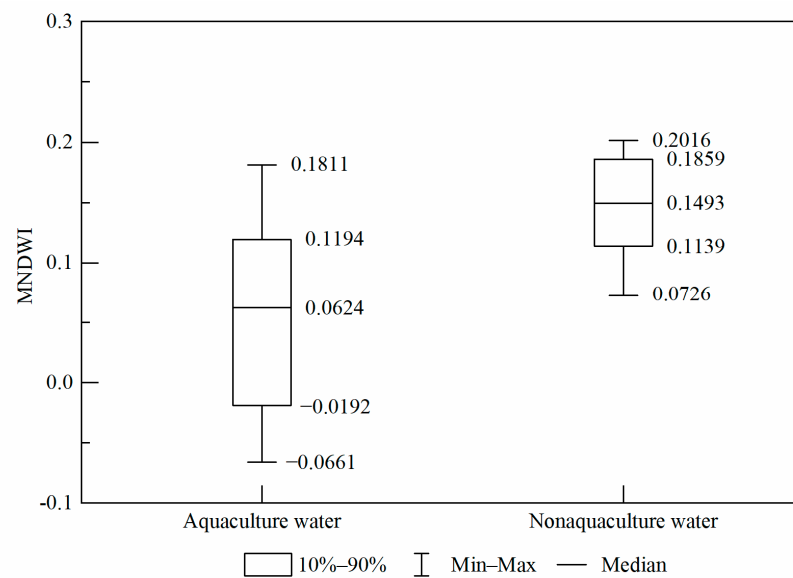
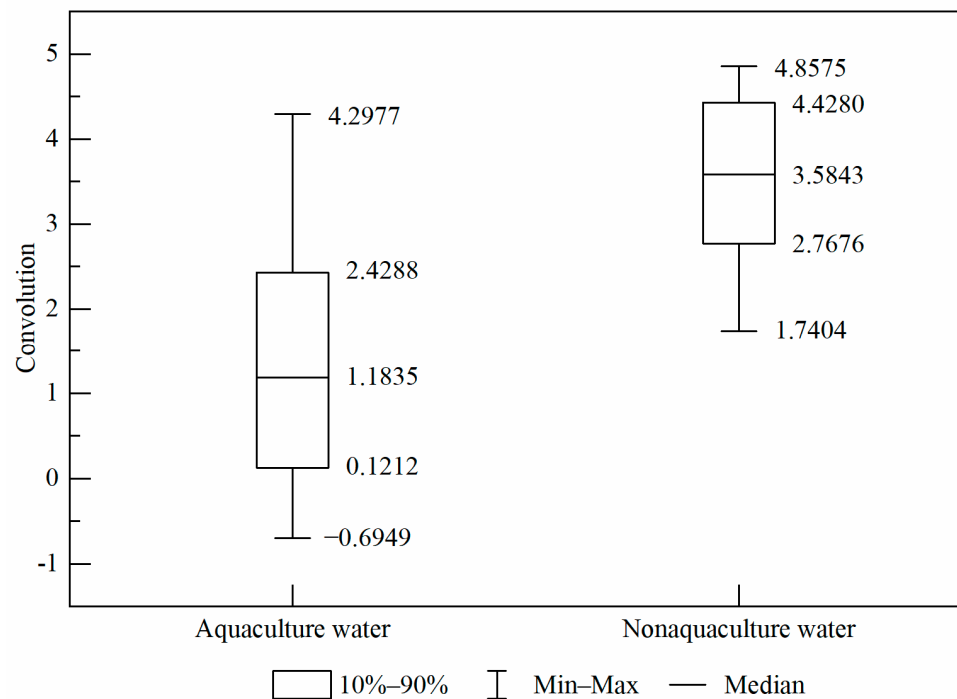


Figure 7. Comparison of MNDWI values between aquaculture and non-aquaculture water bodies in the study area.

To completely distinguish between aquaculture and non-aquaculture water bodies, we used spatial convolution to further increase the spectral differences between these two types of water bodies. We used a  $5 \times 5$  convolution kernel (Formula (3)) to carry out a spatial convolution operation of low-pass filtering on the *MNDWI* exponential image. As with the previous verification, we selected 400 random points for the two types of water bodies from the convolution operation image for numerical statistical analysis (Figure 8). The convolution values of 90% of the aquaculture water bodies were between 0.1212 and 2.4288, and the convolution values of 90% non-aquaculture water bodies were between 2.7676 and 4.4280, effectively separating the two types of water bodies.

$$Kernel = \begin{bmatrix} 1 & 1 & 1 & 1 & 1 \\ 1 & 1 & 1 & 1 & 1 \\ 1 & 1 & 0 & 1 & 1 \\ 1 & 1 & 1 & 1 & 1 \\ 1 & 1 & 1 & 1 & 1 \end{bmatrix} \quad (3)$$



**Figure 8.** Comparison of *MNDWI* convolution values of aquaculture and non-aquaculture water bodies in the study area.

As shown in Figure 9, after *MNDWI* processing, the detailed features of the two types of water were highlighted (Figure 9a,d). The *MNDWI* operation after the convolutional operation further enhanced the low-frequency information of the aquaculture pond, and weakened the internal details of the water, while also obtaining a clear water boundary (Figure 9b,e). The image after convolution was binarized, and the non-aquaculture water area was segmented by the threshold, leaving only the aquaculture water area (the best threshold in the test area was 2.0) (Figure 9c,f).

### 3.4. Postprocessing

Among the previous recognition results, some aquaculture water body regions not filled by morphological closure operation were missing (marked by rectangular boxes in Figure 10a,d). Some non-target redundant water bodies, such as small tributaries or drainage ditches, were mistakenly classified as aquaculture water bodies (marked by circular boxes in Figure 10a,d).

In response to our first research question (i.e., to discover by examination and comparison), the missing holes in the aquaculture water bodies were not attached to the non-aquaculture water bodies. We resolved this issue by turning these holes into entities, and then separating and adding them back to the aquaculture water body areas. Using image spatial difference technology, we could obtain the different images of the water body covering area (Figure 6c,f) and the aquaculture water body covering area (Figure 9c,f) to identify the missing aquaculture water body entities (the rectangular boxes in Figure 10b,e). To address the problem of redundant water bodies, such as tributaries and drainage ditches connected to aquaculture water bodies, we combined visual interpretation and elimination with Google high-resolution images.

After the postprocessing of the recognition result image was completed, we obtained the final range of the aquaculture area (Figure 10c,f).

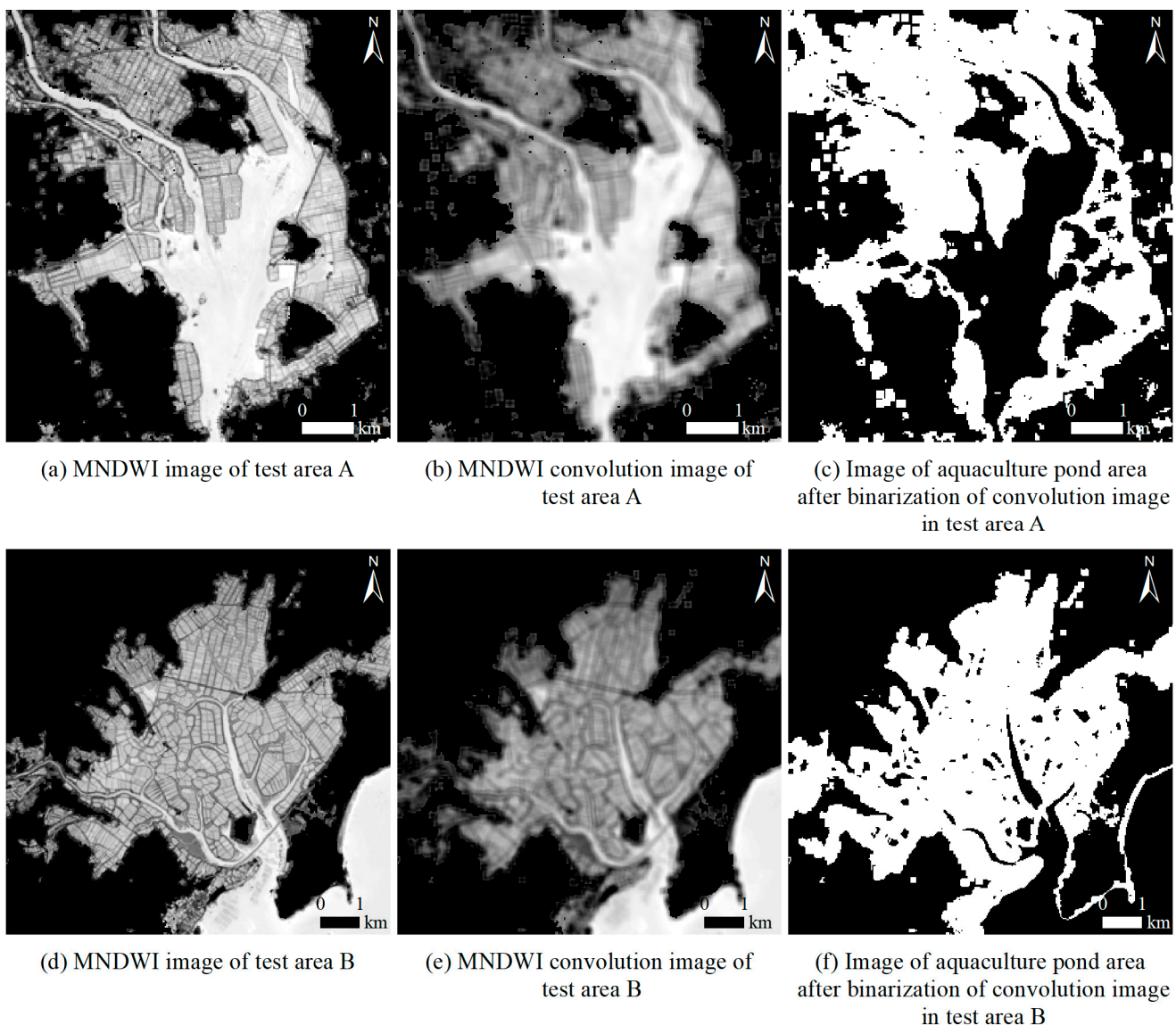


**Figure 9.** Extraction of aquaculture water in test area A (B).

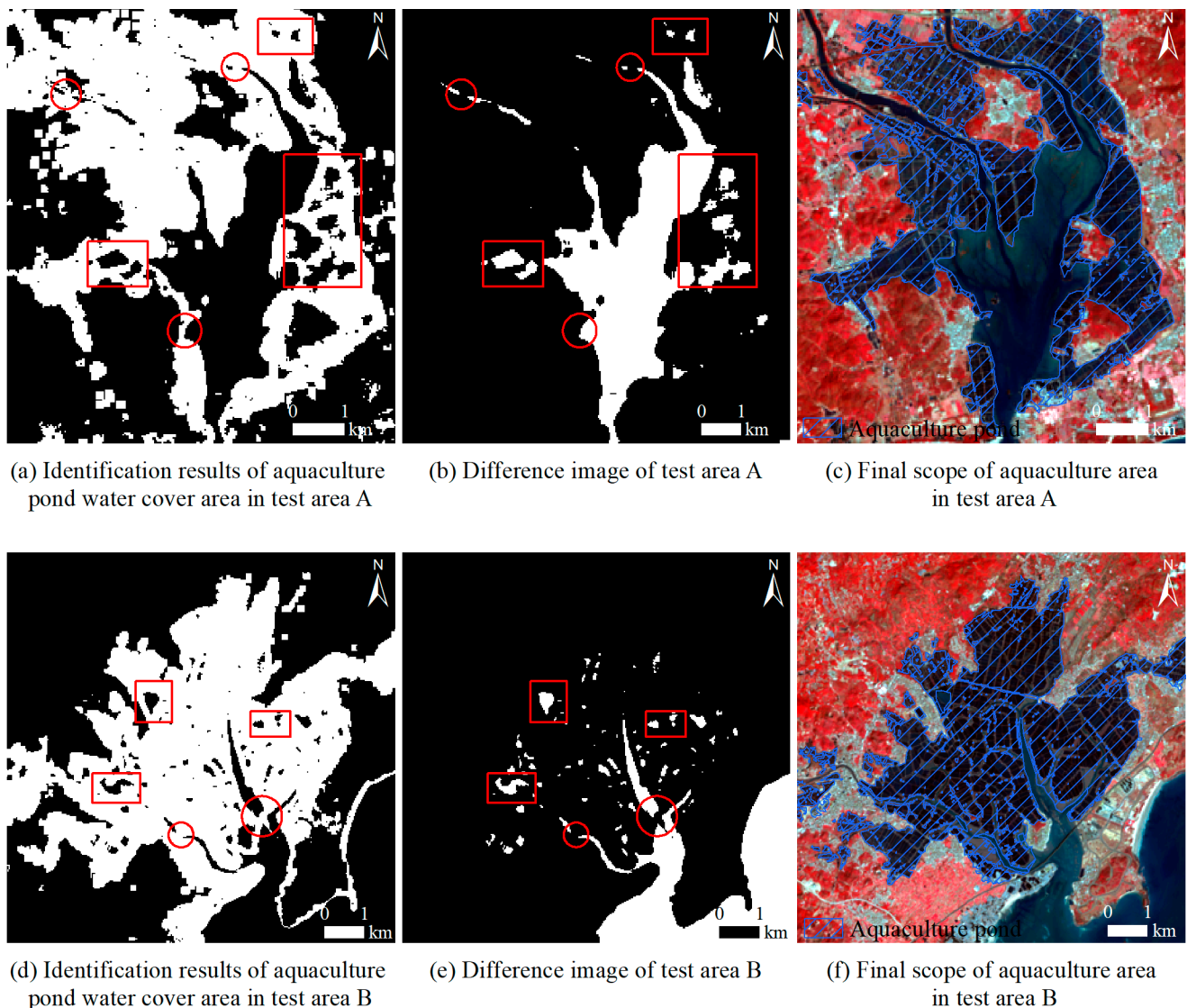


**Figure 10.** Postprocessing of aquaculture water identification results in the test area A (B).

#### 4. Results and Analysis

##### 4.1. Extraction Results and Accuracy Evaluation of Aquaculture Area

We used these methods to identify and extract aquaculture ponds in the coastal areas of southeast China and the main island of Hainan, and obtained a regional distribution map of aquaculture ponds in the coastal areas of southeast China (Figure 11). As shown in Figure 11, the aquaculture ponds in the study area are densely distributed, but their spatial distribution is uneven. The aquaculture ponds in Jiangsu and Guangdong are more distributed and larger in area, and most of the aquaculture areas have a certain scale. In Fujian, Guangxi, and Zhejiang, there are more aquaculture ponds and large-scale concentrated aquaculture zones, but the number is slightly lower than that of Jiangsu and Guangdong. The aquaculture areas in Hainan are small and evenly distributed. Furthermore, the aquaculture areas in the northeast of Hainan have a high degree of agglomeration and scale, whereas the aquaculture ponds in other directions are small in scale. Aquaculture ponds in Shanghai are small in area, are concentrated in distribution and small in scale, and belong to low-density aquaculture areas.

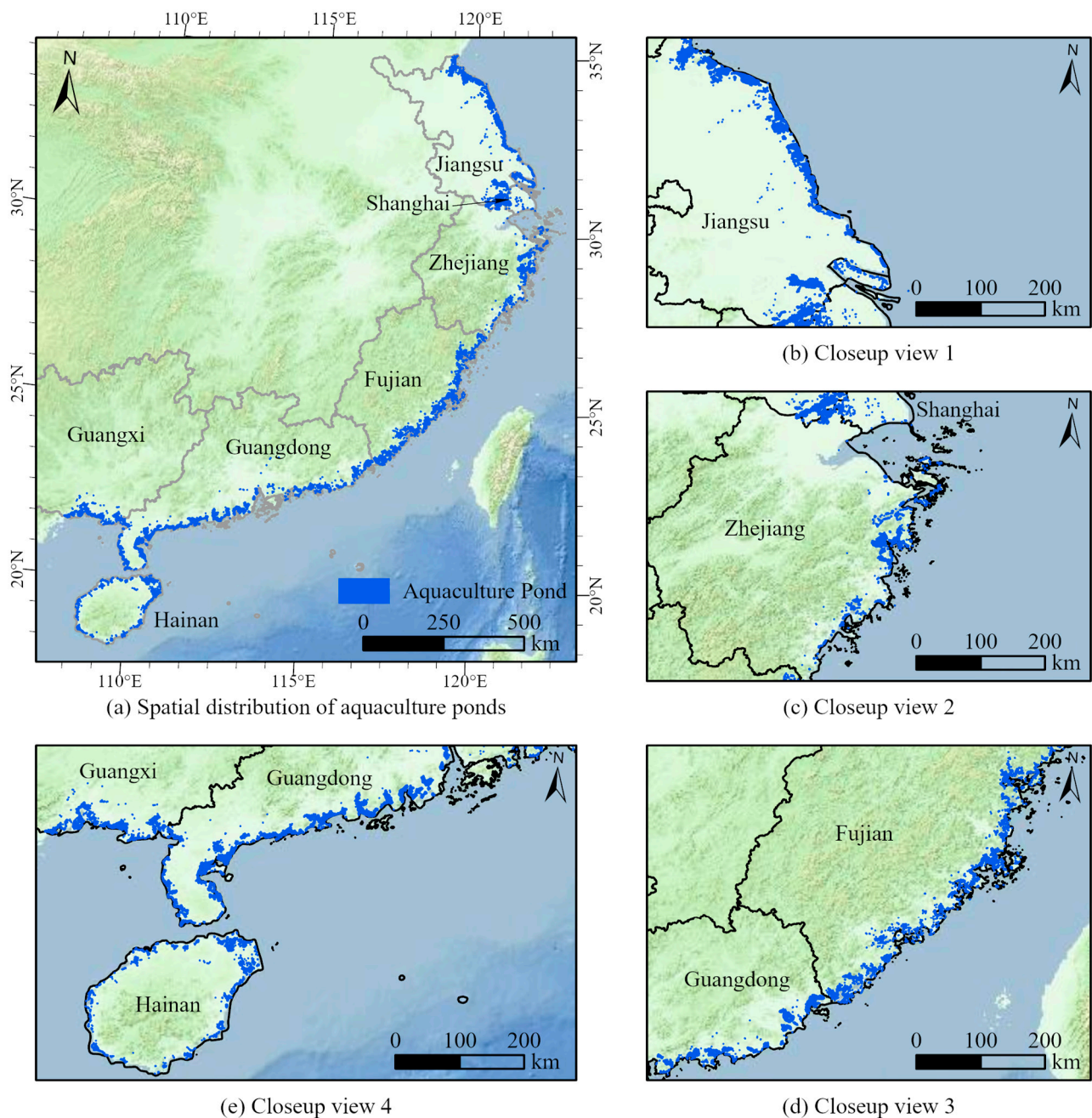


**Figure 11.** Spatial distribution of aquaculture ponds in coastal waters of the southeast region.

To evaluate and test the extraction results, pixels are usually binarized and divided into cultured pond and non-cultured pond areas. Then, verification points are randomly generated, and the accuracy is verified using the confusion matrix and Kappa coefficient. The extraction errors of aquaculture pond areas usually occur at the boundary between water and land, or the junction of different water bodies. If too many random verification points are distributed in the land part that is away from the aquaculture pond areas, it is not possible for the data to play an effective inspection and control role, and it is easy to overestimate the inspection accuracy. Therefore, we designed a restricted random verification point sampling method to replace completely random sampling, and added a typical region stacking comparison test process.

First, random sampling points were generated based on water body information extraction results, and the actual measured points were combined to form a validation data set with a 500-point capacity. Then, we calculated a confusion matrix based on Google's

high-resolution satellite images and field sampling data (Table 1). The test results showed that the extraction method of the aquaculture pond areas in coastal waters combined with spectral features and spatial convolution had high accuracy: the total extraction accuracy reached 93%, and the Kappa coefficient was 0.86.

**Table 1.** Confusion matrix of extraction results.

Attribute Data	Validation Data		User's Accuracy
	Aquaculture Pond Areas	Nonaquaculture Pond Areas	
Aquaculture pond areas	205	27	0.88
Non-aquaculture pond areas	8	260	0.97
Producer's accuracy	0.96	0.91	
Total accuracy = 93%		Kappa = 0.86	

To further test the effectiveness of the extraction method, we added a typical regional overlay comparison test process. Additionally, to calculate the proportion of overlapping areas, based on Google's high-resolution images, we visually interpreted the aquaculture pond areas in test area A (Figure 12c) and test area B (Figure 12b), and conducted a spatial overlay comparison between the visual interpretation results and the automatic extraction results (Figure 12). Test area A is located in Zhangzhou Zhao'an Bay Gongkou port, and test area B is located in Zhangzhou Qianhu Bay. The results showed that the overlap ratio of the automatic extraction results and the visual interpretation results was more than 90% in the two test areas, among which, the overlap ratio of Zhao'an Bay Gongkou port was 91%, and the overlap ratio of Qianhu Bay was 94%. These results further verified the accuracy of the extraction method.

#### 4.2. Spatial Distribution and Density Analysis of Aquaculture Area

According to the extraction results, the total area of aquaculture ponds in the coastal waters of southeast China is 6348.51 km<sup>2</sup>. The area of aquaculture ponds in Guangdong was the largest (2458.60 km<sup>2</sup>), accounting for 38.73% of the total area of aquaculture ponds in the study area. The second-largest area is Jiangsu, with 1858.96 km<sup>2</sup>, accounting for 29.28%. The total area of the two provinces accounted for more than 68% of the total study area. The third largest is Fujian, with an aquaculture pond area of 552.59 km<sup>2</sup>, accounting for 8.70%. Ranked fourth largest is Guangxi, with an aquaculture pond area of 522.87 km<sup>2</sup>, accounting for 8.24%. Zhejiang ranked the fifth largest, with an aquaculture pond area of 490.59 km<sup>2</sup>, accounting for 7.73%. Hainan ranked the sixth largest, with an aquaculture pond area of 402.67 km<sup>2</sup>, accounting for 6.34%. Shanghai was the smallest, with an aquaculture pond area of 62.23 km<sup>2</sup>, accounting for 0.98% (Table 2).

**Table 2.** Aquaculture pond extraction area.

Region *	Extraction Area/km <sup>2</sup>	Percentage/%
Jiangsu	1858.96	29.28
Shanghai	62.23	0.98
Zhejiang	490.59	7.73
Fujian	552.59	8.70
Guangdong	2458.60	38.73
Guangxi	522.87	8.24
Hainan	402.67	6.34
Total	6348.51	100

\* The regions listed in the table are arranged from north to south geographically in the study area's map (Figure 1).

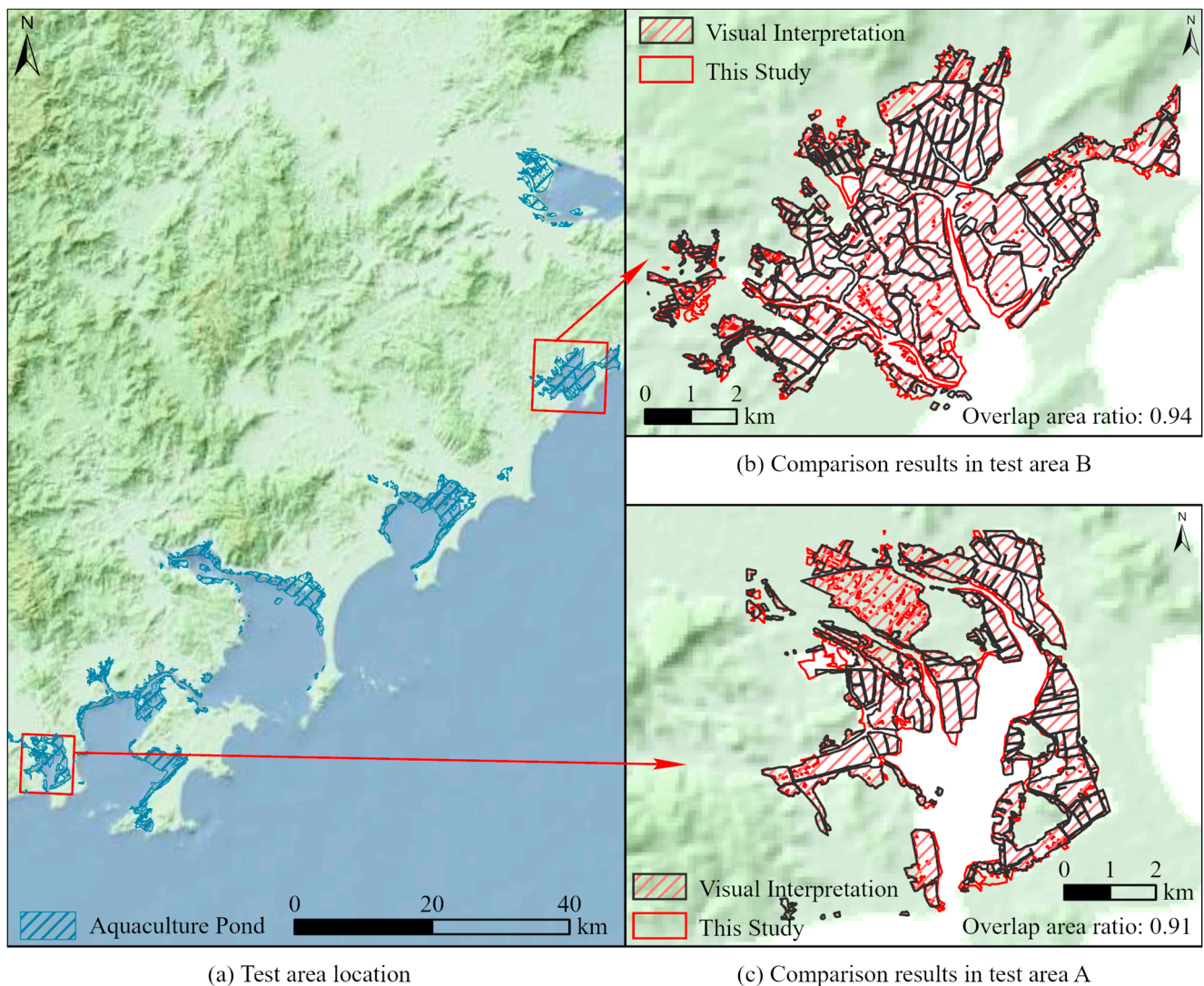


**Figure 12.** Overlapping proportions of results between automated extraction and visual interpretation.

To more intuitively display the spatial concentration degree of aquaculture ponds in the coastal waters of southeast China, we adopted kernel density analysis to represent the density level of each grid in the extraction results by evaluating neighborhood changes (Figure 13). The darker the color was in the image, the higher the spatial concentration degree and density of the aquaculture ponds. Combined with the extraction results of the area of the aquaculture ponds in the coastal waters of southeast China, we found that many areas had high kernel density along the coastline of Jiangsu, indicating that the aquaculture ponds in Jiangsu are densely distributed and large in area. Guangdong has a long coastline, and more than half of the coastline areas belong to the high core density area, indicating that Guangdong has a high concentration of aquaculture ponds and a large area. Therefore, Jiangsu and Guangdong must pay more attention to coastal aquaculture ponds and strengthen aquaculture management. Compared with Guangdong and Jiangsu, Zhejiang, Fujian, Guangxi, and Hainan have lower nuclear density values. Zhejiang has only one high kernel density area, and the rest have low values, indicating that the distribution of aquaculture ponds in Zhejiang is concentrated. Therefore, the management of aquaculture ponds should be strengthened in the high kernel density area. The kernel density values in Fujian are all at the medium level, indicating that aquaculture ponds are widely distributed in Fujian. The extracted area of aquaculture ponds in Guangxi is not significantly different from that in Fujian, but the coastline length of Guangxi is lower

than that of Fujian. Therefore, aquaculture ponds in Guangxi are more concentrated than in Fujian. As shown in Figure 13a, the kernel density value of Guangxi is higher than that of Fujian. Aquaculture ponds are widely distributed in Hainan, but the aggregation degree is low, and the total area is also small. Only one medium kernel density area exists in the northeast region of Hainan, and the rest have low values. Aquaculture ponds in Shanghai are small in area and low in concentration.

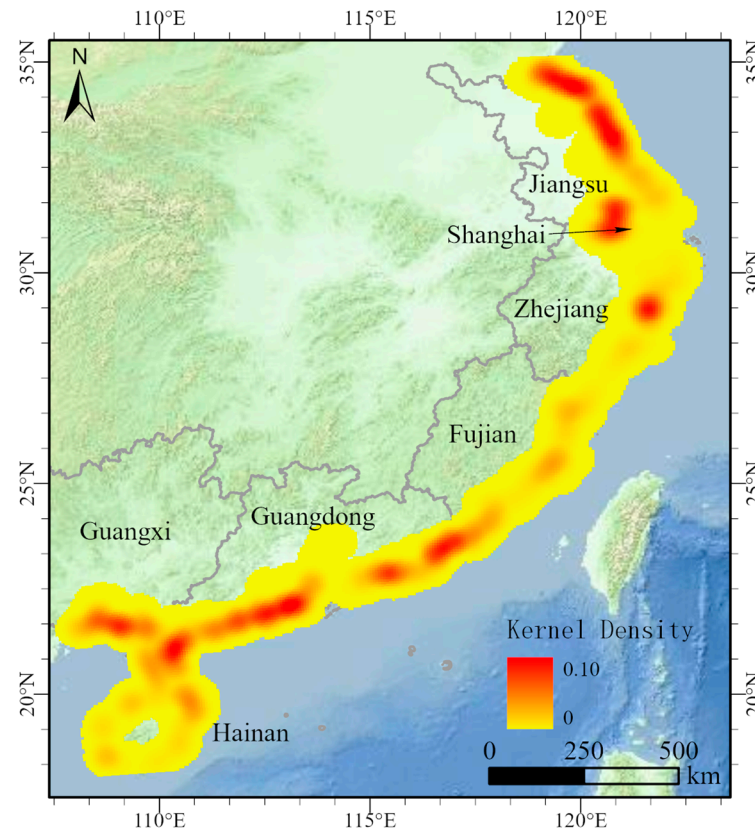


**Figure 13.** Kernel density analysis of the aquaculture pond region in coastal waters of the south-east region.

## 5. Discussion

Based on the extraction results, spatial distribution, and density analysis of the aquaculture area, the management strategy was proposed. It is suggested in the strategy that in the future, in regions such as Guangdong and Jiangsu, the construction of centralized aquaculture tail water treatment facilities is highly recommended, as well as the construction of complete aquaculture facilities, but aquaculture pollution might require more attention. For other regions where the distribution of aquaculture is relatively scattered, it is suggested to integrate the distribution of aquaculture ponds, which should combine with local aquaculture development policies, and to build standard high-quality aquaculture ponds.

Remote sensing technology has become a stable and reliable means of identification and statistics in fishery surveys. An aquaculture pond is the main carrying form of coastal aquaculture. At present, remote sensing recognition and extraction methods can be categorized into three types: visual interpretation, spectral feature, and object-oriented methods. Each method has shortcomings in recognition efficiency, extraction accuracy, data source and operation platform, portability, and robustness. Unlike the remote sensing recognition method that targeted only a single feature category or implemented a single means in previous studies, we proposed a decision-making model for the extraction of aquaculture ponds in coastal waters that combined image spectral information, spatial features, and morphological operations. The main features of this model are as follows:

1. Replace individual extraction with whole recognition. Under the 30 m spatial resolution of Landsat series satellites, the relatively fragmented land patches along the coast, small-scale aquaculture ponds, and dikes constituted a large number of mixed pixels. Thus, it was unrealistic to extract each pit and pond. The extraction of the aquaculture pond area as a whole not only improved the identification accuracy, but also conformed to the attributes of aquaculture land use type. This method met the management needs of the fishery survey on spatial distribution and change statistics of aquaculture ponds at a specific scale.
2. Combine double water spectral indices. In essence, an aquaculture pond is a special water body divided by complex roads and dikes. Therefore, a water spectral index can theoretically realize the identification and extraction of an aquaculture pond, but it was difficult for the traditional single spectral index to achieve large-scale effective separation. *MCIWI* offered the advantage of distinguishing the land–water boundary and highlighting large areas of water (Figure 5), whereas *MNDWI* offered the advantage of distinguishing fine water and highlighting the grid characteristics of aquaculture ponds (Figure 7). The combination of indices made up for the shortcoming of a single spectral index, and effectively realized the separation of aquaculture and non-aquaculture water bodies.
3. Conduct spatial convolution filtering. Spectral characteristics and threshold processing alone cannot distinguish between aquaculture and non-aquaculture water bodies. Based on the network characteristics of aquaculture ponds, which are segmented by roads and dikes, we tested a texture index and a spatial index, and found that after low-pass filtering convolution of the *MNDWI* image, the differences in characteristics between the two types of water bodies can be significantly stretched (Figures 8 and 9). Therefore, this provided good extraction for the aquaculture pond.

This research method addressed the shortcomings of visual interpretation and single spectral features. It can be easily applied to aquaculture pond identification scenarios in other regions with the help of the GEE platform's computing power and massive data sources. It does, however, have the following shortcomings:

1. Under the spatial resolution of the Landsat image and the perspective of provincial scale, the aquaculture pond identified as a whole by region inevitably contains sub-pixel-scale channels and dikes in the region. The width of such ground objects is between 3 m and 10 m. This area is included in the extraction results of the aquaculture pond, which is one of the sources of error.
2. Scattered or small scattered aquaculture ponds interspersed between tidal flats and seawater forms mixed pixels with surrounding features, resulting in misclassification or missing classifications, which is the second source of error.
3. Objective reasons, such as fishermen's irregular pond-clearing behavior and the influence of cloud cover in the optimal collection phase, can lead to the partial probability of a dry pond, and such information is misclassified as land, which is the third source of error.

## 6. Conclusions

In this study, we proposed an automatic extraction method for aquaculture ponds in coastal waters based on image spectral information, spatial features, and morphological operation. This method combined two water spectral indices (*MCIWI* and *MNDWI*) with space convolution to achieve the layered recognition of the land–water boundary and grid characteristics of aquaculture ponds. Replacing individual extraction with overall identification of aquaculture ponds has not only improved the identification accuracy, but also conformed to the attributes of aquaculture land use type. The results of the application in the southeast coastal region of China reflected the high precision and reliability of the extraction method.

With the help of the GEE platform, this method could be applied to other areas in China, providing theoretical reference and data support to reduce both the difficulty of

coastal aquaculture pond management and its negative impact on the environment, and to protect marine water quality.

**Author Contributions:** Y.L. and L.W. conceived the idea; L.W. and Z.L. designed the experiment; Y.L. collected and analyzed the data; Y.L. and D.Z. took the lead in writing the manuscript; L.W., Z.L., Y.L. and D.Z. were involved in the revision of the article. All authors have read and agreed to the published version of the manuscript.

**Funding:** This research was funded by The Key Project of The National Natural Science Foundation of China under grant number U2005205; National Natural Science Foundation of China under grant number 42071300; the Fujian Province Natural Science Foundation Project of China under grant number 2020J01504; China Postdoctoral Science Foundation under grant number 2018M630728.

**Institutional Review Board Statement:** Not applicable.

**Informed Consent Statement:** Not applicable.

**Data Availability Statement:** The data presented in this study are available upon request from the corresponding author.

**Acknowledgments:** The authors would like to thank the National Geographic Information Center of China and National Aeronautics and Space Administration (NASA) of the United States of America for providing support with the observational data. Moreover, we thank the anonymous reviewers for their useful feedback that improved this paper.

**Conflicts of Interest:** The authors declare no conflict of interest.

## References

1. FAO. FAO Yearbook. In *Fishery and Aquaculture Statistics 2018*; FAO: Roma, Italy, 2020.
2. Several Opinions of the State Council on Promoting the Sustainable and Healthy Development of Marine Fishery. Available online: [http://www.gov.cn/zw/gk/2013-06/25/content\\_2433577.htm](http://www.gov.cn/zw/gk/2013-06/25/content_2433577.htm) (accessed on 25 June 2013).
3. Fishery Highlight Serialization in the 13th Five-Year Plan | Accelerating the Transformation and Upgrading in Fishery and Achieving Tangible Results of High Quality Developments. Available online: [http://www.yyj.moa.gov.cn/gzdt/202012/t20201208\\_6357773.htm](http://www.yyj.moa.gov.cn/gzdt/202012/t20201208_6357773.htm) (accessed on 8 December 2020).
4. Fu, Y. Classification of Coastal Mariculture Area and Its Spatial Characteristics in China. Doctoral Thesis, Zhejiang University, Hangzhou, China, 2020.
5. Wu, L.; Yang, S. Discussion on structure optimization and management of aquaculture ecosystem. *Mar. Sci.* **2002**, *26*, 15–17. [[CrossRef](#)]
6. Li, S. Water pollution in inland aquaculture and its control measures. *J. Fish. Sci.* **2005**, *24*, 34–35. [[CrossRef](#)]
7. Chen, L.; Ren, C.; Zhang, B.; Li, L.; Wang, Z.; Song, K. Spatiotemporal Dynamics of Coastal Wetlands and Reclamation in the Yangtze Estuary during Past 50 Years (1960s–2015). *Chin. Geogr. Sci.* **2018**, *28*, 386–399. [[CrossRef](#)]
8. Zhou, M.; Wu, M.; Zhang, G.; Zhao, L.; Hou, X.; Yang, Y. Analysis of Coastal Zone Data of Northern Yantai Collected by Remote Sensing from 1990 to 2018. *Appl. Sci.* **2019**, *9*, 4466. [[CrossRef](#)]
9. Xu, M.; Cui, B.; Lan, S.; Li, D.; Wang, Y.; Jiang, B. Exploring Dynamic Change of the Tidal Flat Aquaculture Area in the Shandong Peninsula (China) using Multitemporal Landsat Imagery (1990–2015). *J. Coast. Res.* **2020**, *99*, 197. [[CrossRef](#)]
10. Jayanthi, M.; Nila Rekha, P.; Kavitha, N.; Ravichandran, P. Assessment of impact of aquaculture on Kolleru Lake (India) using remote sensing and Geographical Information System. *Aquac. Res.* **2006**, *37*, 1617–1626. [[CrossRef](#)]
11. Sun, N.; Zhu, W.; Cheng, Q. GF-1 and Landsat observed a 40-year wetland spatiotemporal variation and its coupled environmental factors in Yangtze River estuary. *Estuar. Coast. Shelf Sci.* **2018**, *207*, 30–39. [[CrossRef](#)]
12. Alonso-Pérez, F.; Ruiz-Luna, A.; Turner, J.; Berlanga-Robles, C.A.; Mitchelson-Jacob, G. Land cover changes and impact of shrimp aquaculture on the landscape in the Ceuta coastal lagoon system, Sinaloa, Mexico. *Ocean. Coast. Manag.* **2003**, *46*, 583–600. [[CrossRef](#)]
13. Gusmawati, N.; Soulard, B.; Selmaoui-Folcher, N.; Proisy, C.; Mustafa, A.; Le Gendre, R.; Laugier, T.; Lemonnier, H. Surveying shrimp aquaculture pond activity using multitemporal VHSR satellite images—Case study from the Perancak estuary, Bali, Indonesia. *Mar. Pollut. Bull.* **2018**, *131*, 49–60. [[CrossRef](#)]
14. Li, F.; Liu, K.; Tang, H.; Liu, L.; Liu, H. Analyzing Trends of Dike-Ponds between 1978 and 2016 Using Multi-Source Remote Sensing Images in Shunde District of South China. *Sustainability* **2018**, *10*, 3504. [[CrossRef](#)]
15. Cui, B.; Zhong, Y.; Fei, D.; Zhang, Y.; Liu, R.; Chu, J.; Zha, J. Floating raft aquaculture area automatic extraction based on fully convolutional network. *J. Coast. Res.* **2019**, *90*, 86–94. [[CrossRef](#)]
16. Cui, B.; Fei, D.; Shao, G.; Lu, Y.; Chu, J. Extracting Raft Aquaculture Areas from Remote Sensing Images via an Improved U-Net with a PSE Structure. *Remote Sens.* **2019**, *11*, 2053. [[CrossRef](#)]

17. Liu, Y.; Yang, X.; Wang, Z.; Lu, C.; Li, Z.; Yang, F. Aquaculture area extraction and vulnerability assessment in Sanduao based on richer convolutional features network model. *J. Oceanol. Limnol.* **2019**, *37*, 1941–1954. [[CrossRef](#)]
18. Nguyen-Van-Anh, V.; Hoang-Phi, P.; Nguyen-Kim, T.; Lam-Dao, N.; Vu, T.T. The influence of satellite image spatial resolution on mapping land use/land cover: A case study of Ho Chi Minh City, Vietnam. In *IOP Conference Series: Earth and Environmental Science*; IOP Publishing: Bristol, UK, 2021; Volume 652, p. 12002. [[CrossRef](#)]
19. Cheng, B.; Liu, Y.; Liu, X.; Wang, G.; Ma, X. Research on Extraction Method of Coastal Aquaculture Areas on High Resolution Remote Sensing Image based on Multi-features Fusio. *Remote Sens. Technol. Appl.* **2018**, *33*, 296–304. [[CrossRef](#)]
20. Huang, S.; Song, K.; Luo, J.; Zhao, J.; Ma, R. A remote sensing extraction algorithm of enclosure culture area in shallow lakes based on gradient transform. *J. Lake Sci.* **2017**, *29*, 490–497. [[CrossRef](#)]
21. Wang, J.; Sui, L.; Yang, X.; Wang, Z.; Liu, Y.; Kang, J.; Lu, C.; Yang, F.; Liu, B. Extracting Coastal Raft Aquaculture Data from Landsat 8 OLI Imagery. *Sensors* **2019**, *19*, 1221. [[CrossRef](#)]
22. Zhang, X.; Ma, S.; Su, C.; Shang, Y.; Wang, T.; Yin, J. Coastal oyster aquaculture area extraction and nutrient loading estimation using a GF-2 satellite image. *IEEE J. Sel. Top. Appl. Earth Obs. Remote Sens.* **2020**, *13*, 4934–4946. [[CrossRef](#)]
23. Sridhar, P.N.; Surendran, A.; Ramana, I.V. Auto-extraction technique-based digital classification of salt pans and aquaculture plots using satellite data. *Int. J. Remote Sens.* **2008**, *29*, 313–323. [[CrossRef](#)]
24. Fu, Y.; Deng, J.; Ye, Z.; Gan, M.; Wang, K.; Wu, J.; Yang, W.; Xiao, G. Coastal aquaculture mapping from very high spatial resolution imagery by combining Object-Based neighbor features. *Sustainability* **2019**, *11*, 637. [[CrossRef](#)]
25. Viridis, S.G.P. An object-based image analysis approach for aquaculture ponds precise mapping and monitoring: A case study of Tam Giang-Cau Hai Lagoon, Vietnam. *Environ. Monit. Assess.* **2014**, *186*, 117–133. [[CrossRef](#)]
26. Disperati, L.; Viridis, S.G.P. Assessment of land-use and land-cover changes from 1965 to 2014 in Tam Giang-Cau Hai Lagoon, central Vietnam. *Appl. Geogr.* **2015**, *58*, 48–64. [[CrossRef](#)]
27. Kang, J.; Sui, L.; Yang, X.; Liu, Y.; Wang, Z.; Wang, J.; Yang, F.; Liu, B.; Ma, Y. Sea Surface-Visible Aquaculture Spatial-Temporal Distribution Remote Sensing: A Case Study in Liaoning Province, China from 2000 to 2018. *Sustainability* **2019**, *11*, 7186. [[CrossRef](#)]
28. Sui, B.; Jiang, T.; Zhang, Z.; Pan, X.; Liu, C. A modeling method for automatic extraction of offshore aquaculture zones based on semantic segmentation. *ISPRS Int. J. Geo-Inf.* **2020**, *9*, 145. [[CrossRef](#)]
29. Liang, C.; Cheng, B.; Xiao, B.; He, C.; Liu, X.; Jia, N.; Chen, J. Semi-/Weakly-Supervised semantic segmentation method and its application for coastal aquaculture areas based on Multi-Source remote sensing images—Taking the Fujian coastal area (Mainly sanduo) as an example. *Remote Sens.* **2021**, *13*, 1083. [[CrossRef](#)]
30. Ren, C.; Wang, Z.; Zhang, B.; Li, L.; Chen, L.; Song, K.; Jia, M. Remote Monitoring of Expansion of Aquaculture Ponds Along Coastal Region of the Yellow River Delta from 1983 to 2015. *Chin. Geogr. Sci.* **2018**, *28*, 430–442. [[CrossRef](#)]
31. Zhang, T.; Yang, X.; Hu, S.; Su, F. Extraction of coastline in aquaculture coast from multispectral remote sensing images: Object-Based region growing integrating edge detection. *Remote Sens.* **2013**, *5*, 4470–4487. [[CrossRef](#)]
32. Gorelick, N.; Hancher, M.; Dixon, M.; Ilyushchenko, S.; Thau, D.; Moore, R. Google Earth Engine: Planetary-scale geospatial analysis for everyone. *Remote Sens. Environ.* **2017**, *202*, 18–27. [[CrossRef](#)]
33. Xia, Z.; Guo, X.; Chen, R. Automatic extraction of aquaculture ponds based on Google Earth Engine. *Ocean. Coast. Manag.* **2020**, *198*, 105348. [[CrossRef](#)]
34. Meilianda, E.; Pradhan, B.; Syamsidik; Comfort, L.K.; Alfian, D.; Juanda, R.; Syahreza, S.; Munadi, K. Assessment of post-tsunami disaster land use/land cover change and potential impact of future sea-level rise to low-lying coastal areas: A case study of Banda Aceh coast of Indonesia. *Int. J. Disaster Risk Reduct.* **2019**, *41*, 101292. [[CrossRef](#)]
35. Chen, D.; Wang, Y.; Shen, Z.; Liao, J.; Chen, J.; Sun, S. Long Time-Series mapping and change detection of coastal zone land use based on google earth engine and Multi-Source data fusion. *Remote Sens.* **2022**, *14*, 1. [[CrossRef](#)]
36. Tew, Y.L.; Tan, M.L.; Samat, N.; Chan, N.W.; Mahamud, M.A.; Sabjan, M.A.; Lee, L.K.; See, K.F.; Wee, S.T. Comparison of three water indices for tropical aquaculture ponds extraction using google earth engine. *Sains Malays.* **2022**, *51*, 369–378. [[CrossRef](#)]
37. Yu, Z.; Di, L.; Rahman, M.S.; Tang, J. Fishpond mapping by spectral and Spatial-Based filtering on google earth engine: A case study in singra upazila of bangladesh. *Remote Sens.* **2020**, *12*, 2692. [[CrossRef](#)]
38. Xu, Y.; Hu, Z.; Zhang, Y.; Wang, J.; Yin, Y.; Wu, G. Mapping aquaculture areas with Multi-Source spectral and texture features: A case study in the pearl river basin (Guangdong), China. *Remote Sens.* **2021**, *13*, 4320. [[CrossRef](#)]
39. Yang, P.; Tan, L.; Huang, J.; He, Q.; Tong, C. Diurnal variations of CH<sub>4</sub> and N<sub>2</sub>O fluxes from the drained aquaculture pond in the minjiang river estuary during early winter. *Environ. Sci.* **2018**, *39*, 300–309. [[CrossRef](#)]
40. Ren, C.; Wang, Z.; Zhang, Y.; Zhang, B.; Chen, L.; Xi, Y.; Xiao, X.; Doughty, R.B.; Liu, M.; Jia, M.; et al. Rapid expansion of coastal aquaculture ponds in China from Landsat observations during 1984–2016. *Int. J. Appl. Earth Obs. Geoinf.* **2019**, *82*, 101902. [[CrossRef](#)]
41. Duan, Y.; Li, X.; Zhang, L.; Liu, W.; Liu, S.; Chen, D.; Ji, H. Detecting spatiotemporal changes of large-scale aquaculture ponds regions over 1988–2018 in Jiangsu Province, China using Google Earth Engine. *Ocean. Coast. Manag.* **2020**, *188*, 105144. [[CrossRef](#)]
42. Duan, Y.; Li, X.; Zhang, L.; Chen, D.; Liu, S.; Ji, H. Mapping national-scale aquaculture ponds based on the Google Earth Engine in the Chinese coastal zone. *Aquaculture* **2020**, *520*, 734666. [[CrossRef](#)]
43. Yang, B.; Chen, F.; Luo, Z. Extraction of complex water information based on MODIS Improved combined water Index (MCIWI). *J. Southwest Univ.* **2011**, *33*, 112–119. [[CrossRef](#)]
44. Otsu, N. A Threshold Selection Method from Gray-Level Histograms. *IEEE Trans. Syst. Man Cybern.* **1979**, *9*, 62–66. [[CrossRef](#)]

45. Zhang, G.; Wu, M.; Wei, J.; He, Y.; Niu, L.; Li, H.; Xu, G. Adaptive threshold model in google earth engine: A case study of ulva prolifera extraction in the south yellow sea, China. *Remote Sens.* **2021**, *13*, 3240. [[CrossRef](#)]
46. Donchyts, G.; Schellekens, J.; Winsemius, H.; Eisemann, E.; van de Giesen, N. A 30 m Resolution Surface Water Mask Including Estimation of Positional and Thematic Differences Using Landsat 8, SRTM and OpenStreetMap: A Case Study in the Murray-Darling Basin, Australia. *Remote Sens.* **2016**, *8*, 386. [[CrossRef](#)]
47. Xu, H. Modification of normalised difference water index (NDWI) to enhance open water features in remotely sensed imagery. *Int. J. Remote Sens.* **2006**, *27*, 3025–3033. [[CrossRef](#)]